

## Attached cavitation at a small diameter ultrasonic horn tip

Anton Žnidarčič,<sup>1,a)</sup> Robert Mettin,<sup>2</sup> Carlos Cairós,<sup>2</sup> and Matevž Dular<sup>1,b)</sup>

<sup>1</sup>Laboratory for Water and Turbine Machines, University of Ljubljana, Aškerčeva 6, 1000 Ljubljana, Slovenia

<sup>2</sup>Christian Doppler Laboratory for Cavitation and Micro-Erosion, Drittes Physikalisches Institut, Universität Göttingen, Friedrich-Hund-Platz 1, 37077 Göttingen, Germany

(Received 7 June 2013; accepted 29 January 2014; published online 27 February 2014)

Ultrasonic horn transducers are frequently used in applications of acoustic cavitation in liquids, for instance, for cell disruption or sonochemical reactions. They are operated typically in the frequency range up to about 50 kHz and have tip diameters from some mm to several cm. It has been observed that if the horn tip is sufficiently small and driven at high amplitude, cavitation is very strong, and the tip can be covered entirely by the gas/vapor phase for longer time intervals. A peculiar dynamics of the attached cavity can emerge with expansion and collapse at a self-generated frequency in the subharmonic range, i.e., below the acoustic driving frequency. Here, we present a systematic study of the cavitation dynamics in water at a 20 kHz horn tip of 3 mm diameter. The system was investigated by high-speed imaging with simultaneous recording of the acoustic emissions. Measurements were performed under variation of acoustic power, air saturation, viscosity, surface tension, and temperature of the liquid. Our findings show that the liquid properties play no significant role in the dynamics of the attached cavitation at the small ultrasonic horn. Also the variation of the experimental geometry, within a certain range, did not change the dynamics. We believe that the main two reasons for the peculiar dynamics of cavitation on a small ultrasonic horn are the higher energy density on a small tip and the inability of the big tip to “wash” away the gaseous bubbles. Calculation of the somewhat adapted Strouhal number revealed that, similar to the hydrodynamic cavitation, values which are relatively low characterize slow cavitation structure dynamics. In cases where the cavitation follows the driving frequency this value lies much higher – probably at  $Str > 20$ . In the spirit to distinguish the observed phenomenon with other cavitation dynamics at ultrasonic transducer surfaces, we suggest to term the observed phenomenon of attached cavities partly covering the full horn tip as “acoustic supercavitation.” This reflects the conjecture that not the sound field in terms of acoustic (negative) pressure in the liquid is responsible for nucleation, but the motion of the transducer surface.

© 2014 AIP Publishing LLC. [<http://dx.doi.org/10.1063/1.4866270>]

### I. INTRODUCTION

Acoustic cavitation is the generation of gaseous voids (cavities, bubbles) in a liquid by an acoustic wave.<sup>1–5</sup> The manifestations of this type of cavitation are typically rather distinct from hydrodynamic cavitation, where the voids are usually created in an unidirectional flow by interaction with a body or a restriction.<sup>6,7</sup> Main reasons for this difference are the repeated excitation and oscillation of acoustic bubbles due to the sound field, and their recirculation in a restricted sonicated volume. Both lead to a complicated long-term dynamics which includes, for instance, rectified gas diffusion<sup>8</sup> and acoustic bubble-bubble interaction.<sup>9–11</sup> In contrast, the hydrodynamic cavitation voids are often

<sup>a)</sup>This research was in part performed while A. Žnidarčič was at Christian Doppler Laboratory for Cavitation and Micro-Erosion, Drittes Physikalisches Institut, Universität Göttingen, Friedrich-Hund-Platz 1, 37077 Göttingen, Germany.

<sup>b)</sup>Author to whom correspondence should be addressed. Electronic mail: [matevz.dular@fs.uni-lj.si](mailto:matevz.dular@fs.uni-lj.si)

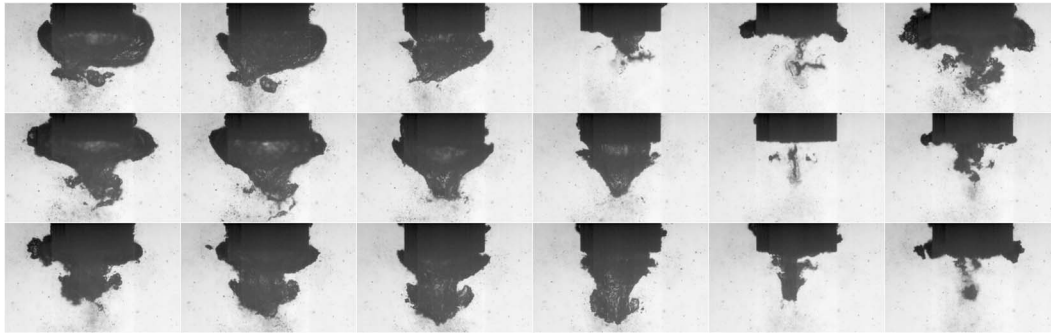


FIG. 1. Three cycles of the oscillation of a large cavity at an ultrasonic horn tip of 3.2 mm diameter in water (Branson sonifier 250, driven at 100 W power, acoustic frequency 20 kHz, recording at 20 000 frames/s, exposure 1  $\mu$ s, sequence row by row from top left). One full acoustic period is passing between each frame, which highlights the subharmonic (slower) oscillation of the large cavity. It collapses after about 6 acoustic cycles, i.e., at approximately 3.3 kHz.

advected with the main flow, show only few oscillations and collapses, and leave the excitation region without being recirculated. An exception is found for “fixed” cavitation,<sup>6</sup> also “attached” or “sheet” cavitation.<sup>4</sup> Then a long-living void is formed directly at a suction surface of the body in the flow. Such cavities can exist quasi-stationary, but in many cases they tend to generate re-entrant jets and to split off bubble clouds in an oscillatory manner.<sup>12–14</sup>

Here, we investigate an acoustically generated cavitation phenomenon which bears some similarities with attached hydrodynamic cavitation, and thus might serve as a test case for better understanding and modeling of both cavitation types. We observed that the tip of an acoustic horn emitter of small diameter and sufficiently large oscillation amplitude can be covered by a single cavity of large extension, i.e., an attached large gas pocket undergoing strong and repetitive expansion-collapse oscillations.<sup>15</sup> The shape is characteristically changing from a “mushroom” form during expansion via a triangular/conical form before implosion into filamentary bubble remnants during collapse. If this extended cavity is present, the horn tip is working most of the time against gas and only in short intervals against liquid. Figure 1 shows an example of three consecutive cavity oscillation cycles. A very peculiar feature is the fact that this large cavitation structure is generating its own oscillation frequency which falls into the subharmonic range of the acoustic excitation frequency  $f_0$  (usually somewhere between  $f_0/7$  and  $f_0/4$ ). The strength of subharmonic acoustic emission generated by the large void can be very pronounced, and its line in an acoustic power spectrum can even overcome the primary wave.<sup>16</sup> Apparently, the emerging frequency does not have to be a small rational fraction of  $f_0$ , unlike other typical subharmonic features in acoustic cavitation spectra.<sup>17,18</sup>

The cavitation at the strongly driven small sonotrode tip is quite distinct to what is observed for lower power or at larger diameter tips.<sup>10,19–21</sup> In the other cases, the attached cavitation directly at the tip is not or is only partially developed, and “streamers” or “clouds” of many individual smaller bubbles occur in the bulk liquid below the horn. These small bubbles show translation, merging, and splitting, and their volume oscillations clearly follow the acoustic driving frequency, as in many other cases of acoustic cavitation.<sup>10</sup> In our setup, populations of small bubbles in the bulk are typically as well present if the large cavity at the tip emerges. They are frequently seen to be ejected from the large cavity during its oscillation.

A visual comparison of various cavitation appearances at horn tips is given in Fig. 2.

The necessary or sufficient conditions for the existence of a large attached cavity or bubble which generates a subharmonic of the driving frequency are not yet clear. Likewise there is still no clear distinction between the “small” and “large” ultrasonic horn tip. The phenomenon could possibly be similar to the transition from the attached to the cloud cavitation in hydrodynamics. There the cavitation first remains attached to the body and oscillates only slightly at a high frequency – as its appearance does not significantly change in time it is also known as steady cavitation type. By the reduction of the system pressure or an increase of the flow velocity, cavitation transits to an unsteady type where large cavitation clouds separate from the attached cavity at a relatively low frequency,

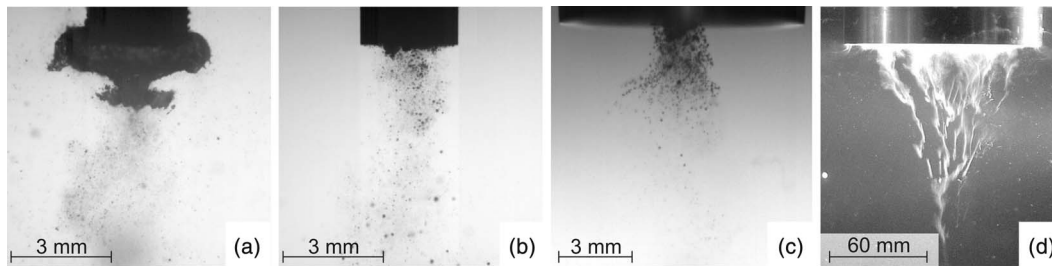


FIG. 2. Examples of visualizations of cavitation at ultrasonic horn emitters at 20 kHz. (a) High power structure at 3 mm diameter horn tip: large attached cavity and small bubbles below; (b) the same horn for lower power: cloud of small bubbles; (c) structure at a larger tip of 10 mm diameter and medium power: small bubble cloud and streamers; (d) very large tip of 120 mm diameter: cone of small bubbles in streamers.<sup>19</sup>

which is usually governed by the Strouhal number

$$Str = \frac{f^* \times d}{v}, \quad (1)$$

where  $f^*$  is the characteristic frequency,  $d$  the characteristic length, and  $v$  the characteristic velocity of the phenomenon. Typical Strouhal numbers associated with the unsteady hydrodynamic cavitation lie in the range between 0.1 and 2 (depending significantly on the choice of characteristic dimensions).<sup>22</sup>

To get more insight into the attached cavitation in the acoustically driven case, a systematic study was performed. We show measurements by a high speed camera and a hydrophone of the dynamics of the attached cavitation on a small ultrasonic horn. Cavitation was observed at different conditions where the presence of gas in the fluid, its viscosity, surface tension, and temperature were altered. In contrast to the experience with other acoustic cavitation systems, the results show that the influence of the fluid parameters is only marginal. Finally, we give some ideas on why cavitation behaves so differently on small and large ultrasonic horns.

## II. EXPERIMENTAL SETUP

The cavitation was produced at the tip of an ultrasonic horn transducer. This type of ultrasound source was first described by Mason<sup>23</sup> and is also called Mason horn, ultrasonic homogenizer, disintegrator, or sonotrode. It consists of a piezo-ceramic element exciting longitudinal waves in a metal rod of reducing diameter and resonant length. The reduced aspect leads to an amplification of the displacement amplitude<sup>24</sup> which is essential for the strong cavitation events at the tip. The horn tip was submerged vertically 1 cm deep into a rectangular glass cell (Hellma,  $5 \times 5 \times 5$  cm<sup>3</sup>) containing water up to a filling height of 4 cm. A high-speed camera was used for observation of cavitation from the side, and in addition acoustic pressure was measured by a hydrophone 7 mm apart. The setup is shown schematically in Fig. 3.

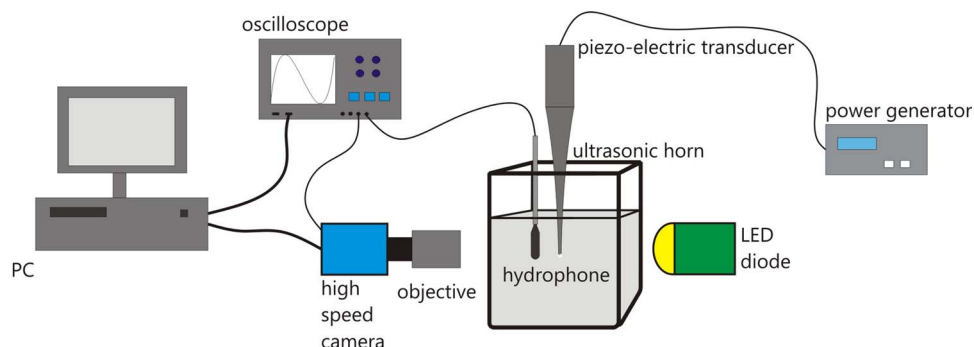


FIG. 3. Experimental setup.

Experiments (except for the one shown in Fig. 1) were run with a Bandelin HD 2070 ultrasonic homogenizer. The horn used is 175 mm long with the tip diameter of 3 mm (MS 73). We determined experimentally that the amplitude of tip vibration changes approximately linearly with the nominal power of the output signal from the electronic generator (GM 2070), which has a peak power of 70 W. At this power the peak to peak amplitude of the tip was 212  $\mu\text{m}$ , measured with help of the camera. The generator's lowest power output is 7 W, at which the tip oscillated with an amplitude of 68  $\mu\text{m}$ . The tip amplitudes appeared essentially independent from the medium the horn was working against, i.e., similar in water and in air. The output signal from the electronic generator has a nominal frequency  $f_0 = 20\,000 \text{ Hz} \pm 500 \text{ Hz}$ .

A high-speed camera (Photron FASTCAM SA5 model 1000K-M1) was equipped with a long distance microscope objective (Infinity Model K2). Using this configuration, it was possible to make recordings of cavitation with 100 000 frames per second (fps) at a relatively high resolution of  $320 \times 184$  pixels. The camera was positioned 330 mm away from the tip and background illumination was provided by a LED diode (Bridgelux BXRA-C4500) which allowed for exposure times down to 1  $\mu\text{s}$ .

A calibrated hydrophone (Reson TC4038, 3 mm diameter) was used for acoustic pressure acquisition. Both the hydrophone and the high-speed camera were connected to an oscilloscope (Tektronix DPO4104) for simultaneous triggering of images and pressure signal.

In addition, a vacuum pump (Frederiksen 0695.25) was used for water degassing, a non-invasive oxygen sensor (PreSens Pst3) could determine the  $\text{O}_2$  saturation level of the water, and a PT100 resistance thermometer was employed for temperature measurement of the liquid.

### III. DATA PROCESSING

#### A. Estimation of the cavitation gas phase volume

For the analysis of the cavitation dynamics, an approximation of the gaseous volume was automatically calculated from the movie frames. As mentioned above, the cavitation at the horn tip occurs in two visually distinct forms: (i) a large coherent gaseous structure directly at the tip which frequently appears like one non-spherical attached bubble, and (ii) much smaller individual bubbles further below, which mainly stream away from the horn tip. Our investigation is focused on the larger attached cavity, which is most of the time the dominant gaseous volume. Therefore, we intentionally suppressed the volume contributions of small individual single bubbles in our evaluation. Due to the background illumination the vapor and gas structures appeared darker than the water in the images, and by setting a brightness threshold (typically 30%) the gas phase was separated from the liquid phase, effectively suppressing the small bubble populations. The volume of the gas phase at the horn was approximated by employing an assumption of partial axial symmetry of the cavitation structures. It was calculated by knowledge of the absolute pixel size and the pixel's distance from the symmetry axis of the horn. Since the cavitation was not completely symmetric, the accuracy of volume estimation was improved by splitting the image along the axis and calculating separately the volume for the left and the right side. Thus, each pixel corresponded to a half ring of vapor. In the final step, the known volume of the horn tip (also dark in the images) was subtracted from the calculated cavitation gas volume. A complete correction for the oscillatory tip motion was not feasible, and thus a small modulation of the measured gas volume by this artifact might be possible. With the described procedure the gas volume of the large attached cavity is correctly obtained if it is axi-symmetric and concave, i.e., no liquid phase is hidden inside the dark structure. Due to the just mentioned assumptions the obtained volume can only be seen as a rude approximation of the real one (we can only claim that the value we determine is in a relative relationship with the "real" cavity volume).

#### B. Pressure calculation

The signal from the hydrophone was recorded in terms of voltage. The measured signal was calibrated according to the amplification and to the nominal sensitivity of the hydrophone

( $n_s = -228$  dB) to give the results in terms of pressure (Pa). The sampling rate of 1 MHz could well resolve the pressure peaks from the large cavity collapse. The uncertainty of pressure measurements was estimated to  $\pm 10\%$  of the measured value.

### C. Determination of the cavity oscillation frequencies

The frequency of cavity oscillations was obtained by Fast Fourier Transform of both the pressure and cavity volume data. It could be determined relatively exactly since a large ensemble of data was recorded. In case of pressure measurements, we estimate the uncertainty to  $\pm 1$  Hz and in the case of the cavity size to  $\pm 4$  Hz.

## IV. RESULTS

All results that follow were recorded with the Bandelin horn. As explained above, we concentrate on the dynamics of the large coherent attached cavitation structure. For variations of power and liquid parameters, we recorded synchronously high-speed movies and hydrophone signals. Representative sections of gas volume and pressure vs. time over 3 ms length are shown, together with some typical movie frames.

### A. Reference cavitation at different powers

As a part of preliminary tests we investigated how the behavior of the attached cavitation changes when the ultrasonic horn operates at different powers. For sufficiently low powers (below 20%), the large cavity does not occur, and only small bubbles appear, cf. Fig. 2(b). With the large cavity being present, three tests were performed – at 30%, 50%, and 70% of maximal power (70 W) what corresponds to amplitudes of the tip of 100, 132, and 164  $\mu\text{m}$ , respectively. The liquid used was distilled water saturated with air at temperature of 23 °C. The diagrams in Figs. 4–6 show time evolutions of pressure and the estimated volume of the attached cavitation bubble. On the top, a sequence of images captured every 30  $\mu\text{s}$  is shown. The full recording was taken at 100 000 frames/s, i.e., with an inter-frame interval of 10  $\mu\text{s}$ , and with an exposure time of 1  $\mu\text{s}$ . The six frames presented roughly cover a complete oscillation cycle of the large cavity between two subsequent collapses.

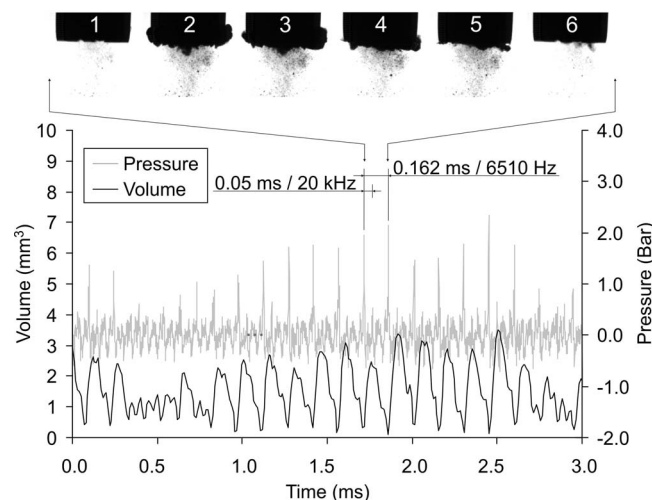


FIG. 4. Time evolution of pressure and the size of the attached cavity at 30% power. The sequence of images on top covers the marked interval with an inter-frame interval of 30  $\mu\text{s}$ .

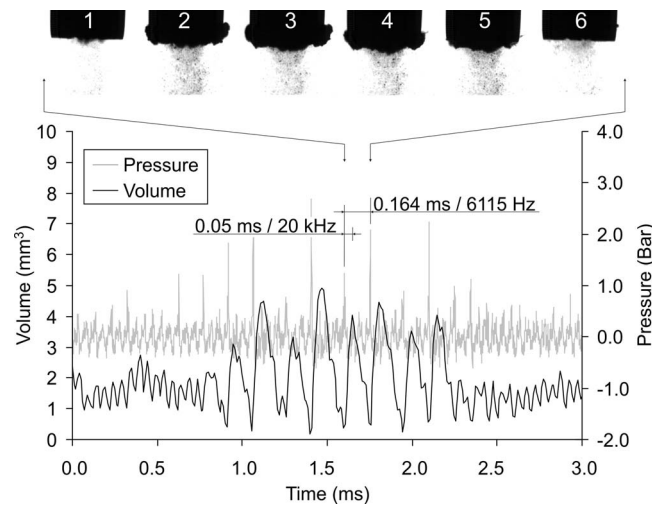


FIG. 5. Time evolution of pressure and the size of the attached cavity at 50% power. The sequence of images on top covers the marked interval with an inter-frame interval of  $30 \mu\text{s}$ .

As expected the maximum cavitation structure volume grows when the power is increased. One can see that as the large cavity implodes (as the volume rapidly shrinks), always a pressure peak is measured by the hydrophone. Sometimes also a multiple peak is resolved.

The length of the cavitation cycle (one growth and collapse of the large attached cavity) also increases (its frequency decreases) with added power. Typical frequencies are about 6.5 kHz at 30%  $P_{\text{max}}$ , 6.1 kHz at 50%  $P_{\text{max}}$ , and 5 kHz at 70%  $P_{\text{max}}$ . Thus, the attached cavity oscillation period at 30% and 70% of  $P_{\text{max}}$  roughly corresponds to 3 and 4 oscillations of the ultrasonic horn tip, respectively. The self-generated subharmonic frequency at 50% power corresponds to about 3.3 tip oscillations. It is somewhat less pronounced, and the large cavity oscillation period frequently shifts between regimes of 3 and 4 acoustic cycles. In between, the dynamics can become irregular or even disappears. The reason might be the inability of the cavity oscillation to fully entrain or “lock” to either 3 or 4 acoustic cycles. This is a typical phenomenon of periodically driven self-excited oscillators<sup>25,26</sup> and is further indication of the auto-generation of the large cavity’s frequency.

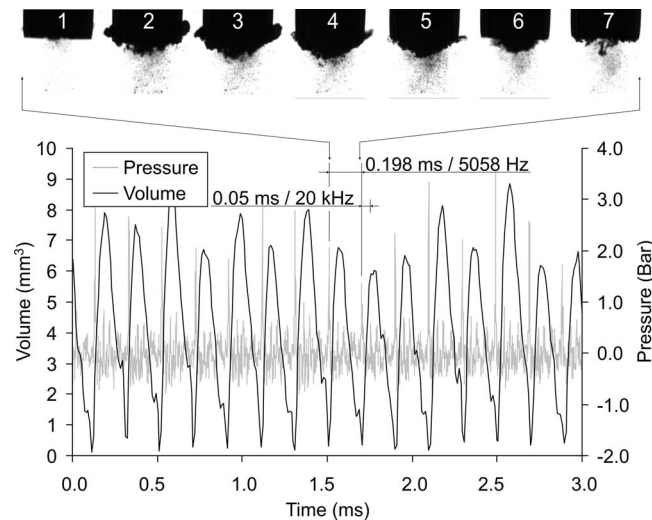


FIG. 6. Time evolution of pressure and the size of the attached cavity at 70% power. The sequence of images on top covers the marked interval with an inter-frame interval of  $30 \mu\text{s}$ .

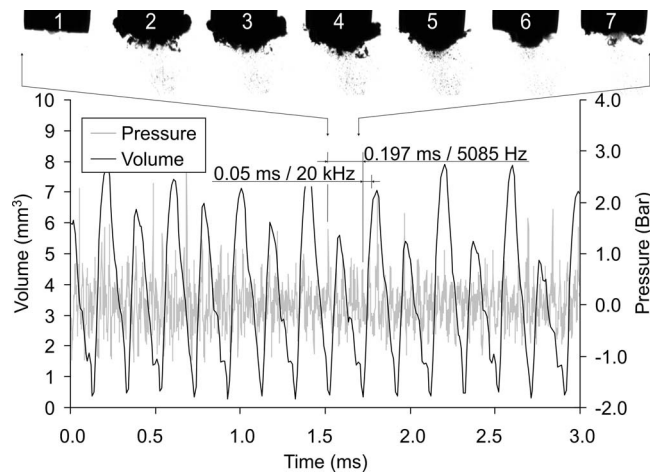


FIG. 7. Time evolution of pressure and the size of the attached cavity at 70% power for lower air saturation level (50%). The sequence of images on top covers the marked interval with an inter-frame interval of  $30 \mu\text{s}$ .

Another interesting and peculiar phenomenon of the driven oscillator system can be perceived in Fig. 6 (and later even more pronounced in Fig. 7), namely, a period doubling:<sup>25</sup> the cavity's maximum expansion is alternating from cycle to cycle.

While the acoustic power changes the cycle length and the size of the attached cavitation, the basic physics seems to remain the same: a large cavity emerges and does not follow the oscillation of the ultrasonic horn, but oscillates at a reduced frequency. It partly covers the full tip and performs a characteristic shape sequence during expansion and collapse. Due to limitation of the space and assuming the same physical background, we present only results at 70%  $P_{\text{max}}$  in Sec. IV B.

## B. Parameter variations

The main goal of the study was to investigate the liquid parameters which could influence or explain the peculiar dynamics of cavitation on the small ultrasonic horn. Thus, besides the power of the ultrasonic transducer, we tested the influence of:

- Presence of gas in the liquid: In the reference experiment, we used filtered water (free of solid particles) which was saturated with air. Degassing the water is expected to reduce or suppress bubble nucleation and consequently also cavitation.
- Viscosity: It might influence the intensity of the turbulence and consequently also cavitation, as the pressure can locally drop below vapor pressure inside the eddies.
- Surface tension: It is expected to influence the critical amplitude of acoustic pressure at which cavitation nuclei begin to rapidly grow into bubbles. Also a change of surface tension might – as viscosity – influence the splitting and disintegration of larger bubbles.
- Temperature: On one hand, the increase of temperature leads to increase of vapor pressure and by this to the conditions more prone to cavitation. On the other hand, the theory of the so called “thermal delay” states that more evaporation heat is needed for bubble growth at higher temperature since the density of vapor is higher. This would result in reduced cavitation size. However, this effect is expected to become significant only when the liquid temperature nears the critical point ( $373.9^\circ\text{C}$  for water). There will also be indirect changes of viscosity, surface tension, and density due to the variation of the temperature. The experiments were conducted in a way to minimize these indirect effects.

All tests presented in this article are summed in Table I (without the geometry controls discussed in Sec. IV C).

Test number 3 presented in Fig. 6 (water saturated with air at  $23^\circ\text{C}$  and 70% power) is considered a reference test and is therefore shown in bold letters.

TABLE I. Tested variables and ranges. Test number 3 is considered a reference test and is therefore shown in bold letters).

Test	Fluid	P (%)	T (°C)	Sat. (%)	$\mu$ (Pa s)	$\sigma$ (N/m)	$\rho$ (kg/m <sup>3</sup> )	$p_v$ (Pa)	Fig.
1	H <sub>2</sub> O	30	23	100	0.000932	0.072	998	2808	4
2	H <sub>2</sub> O	50	23	100	0.000932	0.072	998	2808	5
<b>3</b>	<b>H<sub>2</sub>O</b>	<b>70</b>	<b>23</b>	<b>100</b>	<b>0.000932</b>	<b>0.072</b>	<b>998</b>	<b>2808</b>	<b>6</b>
4	H <sub>2</sub> O	70	23	50	0.000932	0.072	998	2808	7
5	H <sub>2</sub> O	70	23	20	0.000932	0.072	998	2808	8
6	H <sub>2</sub> O+SDS	70	23	100	0.000932	0.05	998	2808	10
7	C <sub>2</sub> H <sub>6</sub> O <sub>2</sub>	70	23	100	0.0169	0.048	1115	7.5	11
8	C <sub>3</sub> H <sub>8</sub> O <sub>3</sub>	70	23	100	1.499	0.0634	1261	0.333	12
9	H <sub>2</sub> O	70	45	100	0.000596	0.069	990	9584	13
10	H <sub>2</sub> O	70	65	100	0.000433	0.065	981	25015	14

Results of tests (Figs. 7–14) are shown again in the same way as before: time evolutions of the pressure and the estimated volume of the attached cavity are presented for a typical section of the recordings, and a sequence of images covering one typical and indicated cavity cycle is given on the top.

### 1. Saturation with air

As already mentioned the quantity of the dissolved gases (here air) in the liquid might influence the cavitation and its dynamics. In the reference experiment (Fig. 6), the water was saturated with air. We decreased the air content by vacuuming the water sample until we reached 50% (Fig. 7) and 20% saturation (Fig. 8). All other parameters remained the same as in the reference experiment (Table I).

At 50% saturation the cavitation dynamics remained practically the same as in the reference experiment. One could expect the structures to be slightly smaller, but their volume practically did not change. The frequency increased slightly, but one can still perceive a good locking to 1/4 of the driving frequency at approximately 5 kHz. A distinct period doubling of the volume maxima occurs at times.

The maximum pressure peaks do not change, but the negative amplitudes are somewhat larger – up to  $-0.7$  bar in the reference experiment and  $-1.0$  bar in the present case. This is probably due

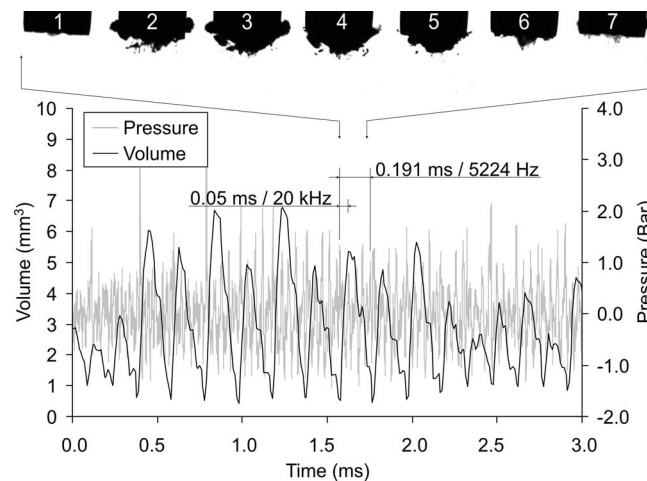


FIG. 8. Time evolution of pressure and the size of the attached cavity at 70% power for the lowest investigated air saturation level (20%). The sequence of images on top covers the marked interval with an inter-frame interval of 30  $\mu$ s.



FIG. 9. Images of cavitation cloud for the lowest saturation level (20%) at startup (images with inter-frame interval of  $20 \mu\text{s}$ ).

to smaller amount of tiny cavitation structures and bubbles between the horn and the hydrophone (see cavitation images in Figs. 6 and 7), what results in smaller attenuation of the pressure waves.

As expected (due to increasing tensile strength of the water), when the gas content was decreased even further (to 20%, Fig. 8) the attached cavitation structures did not reach the same size as before. Consequently, the cavitation cycle accelerated a bit – to about 5.2 kHz. Similarly, the pressure peaks do not reach the same amplitudes and their maximal negative values increase even more – to about  $-1.5 \text{ bar}$ .

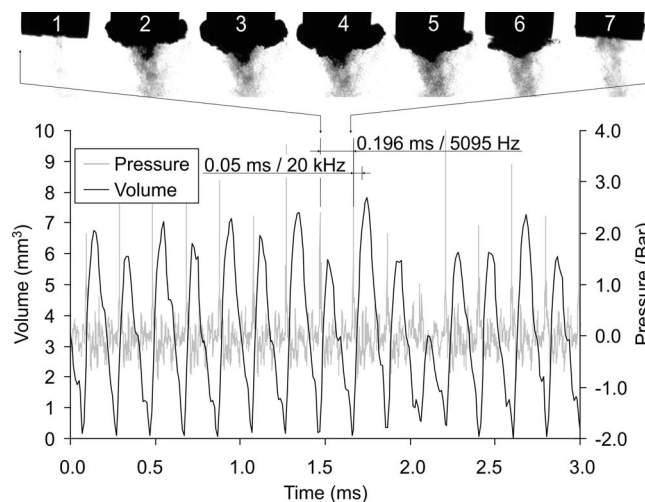


FIG. 10. Time evolution of pressure and the size of the attached cavity at 70% power for lower surface tension ( $0.05 \text{ N/m}$  by addition of  $0.5 \text{ g/l}$  SDS). The sequence of images on top covers the marked interval with an inter-frame interval of  $30 \mu\text{s}$ .

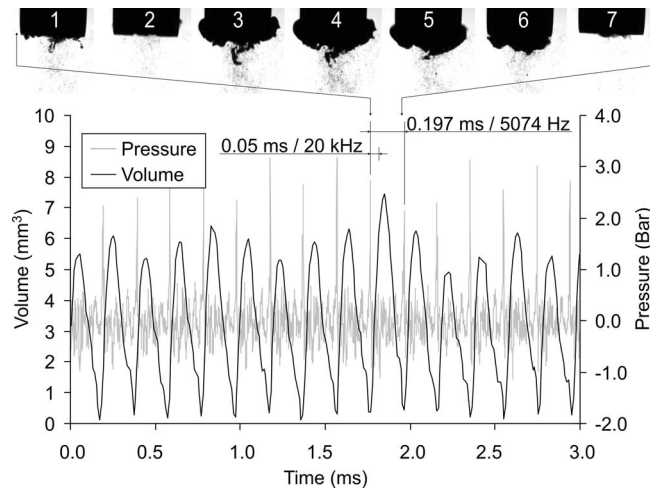


FIG. 11. Time evolution of pressure and the size of the attached cavity at 70% power for higher viscosity (0.0169 Pa·s; ethylene glycol). The sequence of images on top covers the marked interval with an inter-frame interval of 30  $\mu$ s.

At the initial stages of the test with very low gas content (the first 1 ms), one could observe the influence of the presence of cavitation nuclei on the emergence of the large attached cavitation structure (Fig. 9).

At first no (or very few) nuclei are present due to the low gas content. As the negative pressure finally exceeds the tensile strength of water (defined by the largest nucleus) it breaks and the first bubble appears at the edge of the tip (image no. 6 in Fig. 9). The bubble then grows and breaks into smaller bubbles which act as further cavitation nuclei, decreasing the overall tensile strength of the water. Subsequently, more and more bubbles appear from fission, and finally (after less than 1 ms or approximately after 15 oscillations of the horn) cavitation exhibits the same behavior as in the cases with larger gas content. In the case of higher air content, the initial transient is much shorter and of the order of just a few tip oscillations.

If one compares the results to past works in hydrodynamic cavitation some similarities can be found. It was shown that the number of nuclei influences the hydrodynamic cavitation in incipient stage.<sup>27</sup> The dependency for the case of larger (developed) cavitation is less investigated – it was, for

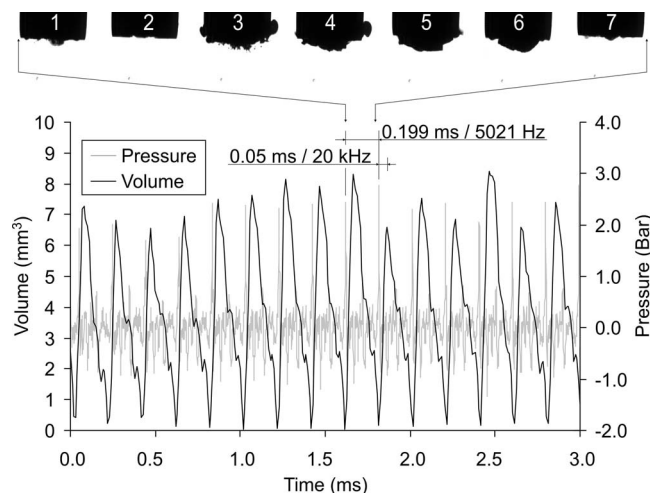


FIG. 12. Time evolution of pressure and the size of the attached cavity at 70% power for the highest viscosity (1.499 Pa·s; glycerol). The sequence of images on top covers the marked interval with an inter-frame interval of 30  $\mu$ s.

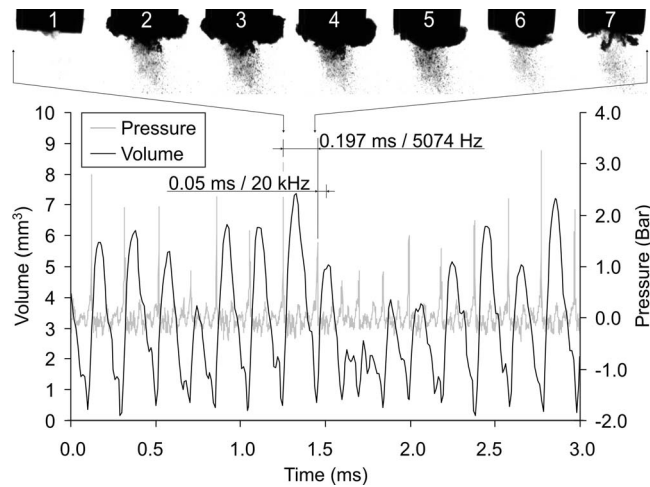


FIG. 13. Time evolution of pressure and the size of the attached cavity at 70% power for higher temperature of 45 °C. The sequence of images on top covers the marked interval with an inter-frame interval of 30  $\mu$ s.

example, found that the cavitation in saturated water has a less pronounced dynamics and a slightly larger extent.<sup>28</sup>

## 2. Surface tension

We added a small amount (0.5 g/l) of sodium dodecyl sulfate (SDS) to the water to decrease its surface tension to 0.05 N/m. Since a very small amount of SDS was added, the other properties of the fluid remained the same.

All characteristics, i.e., the size of the structures, the amplitude of the pressure oscillations, and the frequency of the attached cavitation cycle did not significantly change compared to the reference experiment (Fig. 6). The only difference is the larger amount and reduced size of the isolated tiny bubbles beneath the tip of the horn, which corresponds to previous results for acoustic cavitation.<sup>29,30</sup> This apparently results from the breakup of larger bubbles which is easier due to the lower surface tension, and possibly from modified close range interaction between bubbles and hampered coalescence.<sup>31</sup>

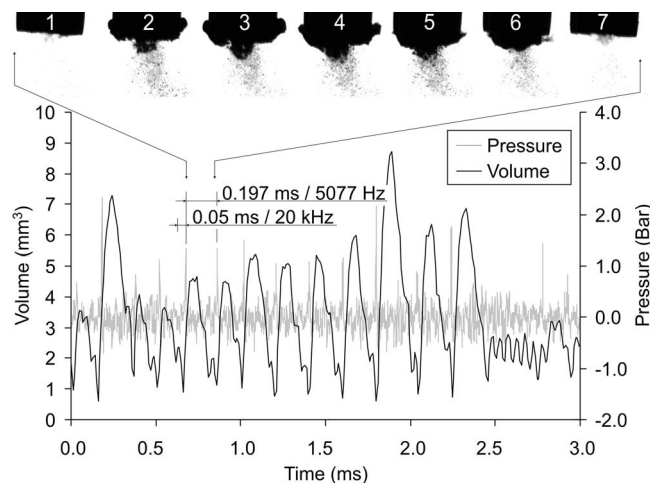


FIG. 14. Time evolution of pressure and the size of the attached cavity at 70% power for the highest temperature of 65 °C. The sequence of images on top covers the marked interval with an inter-frame interval of 30  $\mu$ s.

Similar conclusions were also drawn for the case of hydrodynamic cavitation,<sup>32,33</sup> where it is argued that at the conventional (large) scale, surface tension impacts the bubble growth only in the initial stages. Once the bubble reaches a substantial size, the influence of the surface tension diminishes. Hence, in most cases and particularly in industrial situations, it is a good approximation if one assumes that it does not influence the main characteristics of cavitating flow.

### 3. Viscosity

The viscosity of the liquid influences the intensity of the turbulence and consequently also cavitation, as the pressure can locally drop below vapor pressure inside the eddies. Also the dissipation by the oscillating bubbles and their stability against splitting should increase with viscosity. Two tests with ethylene glycol ( $C_2H_6O_2$ ) and glycerol ( $C_3H_8O_3$ ) were performed. Their density, viscosity, vapor pressure, and surface tension are different from those of water, see Table I. As we have seen from the previous test (Fig. 10), however, we can mainly neglect the influence of the decrease of the surface tension. The density differences in the range of 20% against water should also not be significant. The vapor pressure is further reduced as compared to water and is almost negligible with relation to the atmospheric pressure. Thus, it should not change the main bubble dynamics, but might lead to impeded nucleation and more intense pressure peaks or shocks, as the collapse is less “cushioned” by non-condensed vapor. The parameter that is changed most significantly is the viscosity, as it increases by a factor of about 15 and 1500, respectively. Therefore, one can expect that observed differences in attached cavitation dynamics will be due to the altered liquid viscosity.

The results are shown in Figs. 11 and 12. Again, no dramatic changes occur. The attached cavities expand slightly less than in the reference experiment, which is probably a direct result of the increased dissipation in the higher viscosity liquids. Still, the oscillation frequency stays close to 5 kHz and the shape appears similar to the water case. The collapse pressure peaks indeed appear more pronounced for ethylene glycol (but not for glycerol), which might be contributed to the lower vapor pressure.

Another observation is the reduction or even disappearance (for glycerol, Fig. 12) of tiny bubble cavitation structures beneath the horn. We attribute this, on the one hand, to the increased viscosity which attenuates the growth of the bubbles and their breakup due to smaller turbulence level. On the other hand, the lower vapor pressure increases the tensile strength of the fluid and hampers nucleation in the bulk liquid. As a result, also the negative pressure peaks in the acoustic signals are larger, because bubbles do not scatter or attenuate the pressure signal as it travels from the horn to the hydrophone. This effect is more pronounced for glycerol.

In conclusion, we do not see substantial influence of viscosity on the emergence and dynamics of the attached cavitation at the horn tip.

Effects of viscosity in hydrodynamic cavitation were studied recently.<sup>34</sup> There hydrodynamic cavitation in water and glycol was compared. It was found that the hydrodynamic cavitation in glycol is less homogeneous than in water and that it starts further downstream on a foil – due to the presence of a laminar separation bubble. Cavitation also appeared thicker and longer in less viscous fluid, what, to some extent, complies with our findings on an ultrasonic horn.

### 4. Temperature

To study the influence of the water temperature, we increased it to 45 °C (Fig. 13) and 65 °C (Fig. 14), respectively. The main influence is expected from the increased vapor pressure which rises to 9584 Pa and 25 015 Pa, corresponding to about 10% and 25% of air pressure, respectively. Higher vapor pressure results in conditions more prone to cavitation. Additionally, the collapse pressures should reduce due to cushioning by vapor.

The results in Fig. 13 show that neither the size of cavitation structures nor the averaged frequency changed dramatically. However, one observation is that the main oscillation frequency is not as pronounced as before – sometimes the attached structures appear and collapse faster and sometimes slower (see, for example, the four evolutions of the cavity volume between 1.5 and 2 ms in Fig. 13). Thus, we notice a larger frequency jitter in the cavity’s cycle. This is probably due to the fact that the conditions for appearance of the cavity are easier to achieve which results in

more random occurrence of the cavitation. Both the pressure maxima and minima appear reduced as compared to the reference experiment, which might be attributed to a higher number density of small bubbles in the liquid (as a consequence of decreased tensile strength and amplified nucleation rate) and higher vaporization pressure. The collapse peaks do not reach the high values of the reference, which is in accordance with a larger cushioning by vapor. It can also be seen that the minimum gaseous volume is elevated, i.e., the collapsed volume (up to resolution) stays finite. This might be contrasted with the lowest vapor pressure case of glycerol (Fig. 12).

Figure 14 shows that the experiment at 65 °C confirmed and amplified the results from the one at 45 °C. The attached cavity oscillates somewhat more randomly, but in average the frequency stays the same at about 5 kHz. The pressure peaks decrease even more than at 45 °C, and we see again reduced negative parts of the acoustic signal.

Besides a higher frequency jitter and somehow “softened” oscillations, the experiments did not reveal a significant temperature effect on the attached cavity dynamics. As expected, no influence of the so called “thermal delay” was observed as the temperature of the water stayed well below the critical one.

It was observed in hydrodynamic cavitation that at a higher free stream temperature and a constant cavitation number the cavity length is smaller and is initiated at a higher cavitation number.<sup>35</sup> On the other hand, the results of other studies<sup>36</sup> show just the opposite – at elevated temperature the cavity becomes thicker and longer. No clear reason behind this discrepancy was yet offered although it was suggested that the constraints of the channel might play a significant role. With this in mind and due to the obvious geometrical differences of hydrodynamic and acoustic cavitation the similarity of the physics behind the two cases in terms of the temperature influence cannot be drawn.

### C. Influence of the setup geometry

Finally, we tested the influence of the geometry of the experimental setup on the dynamics and size of cavitation, namely, the distance of the ultrasonic horn tip from the bottom of the cuvette and the liquid filling height. Positioning the ultrasonic horn tip too close to the bottom of the cuvette will break up the circular flow around it<sup>16</sup> and consequently influences the cavitation dynamics. This creation of a too narrow gap under the horn was avoided. The quantity of water, on the other hand, shifts the resonance frequencies of the cuvette system (not of the driving horn), and thus an influence could be checked. The distance of the tip from the bottom was reduced from 30 mm (the reference height) to 15 mm, and the filling height of the fluid lowered from the reference level of 4 cm to 3 cm. Measurements were performed at 70% power at 23 °C in filtered water saturated with air.

When the tip was moved to the closer distance of 15 mm to the bottom of the cuvette, the attached cavity became a bit larger (about 5% difference was determined between the distances of 15 and 30 mm). The frequency of the cavity oscillation, on the other hand, remained constant at approximately 5 kHz.

Changing the height of the fluid did not influence the observed cavitation at all. The lowest resonance of the water filled cuvette, the (1,1,1) mode, lies approximately at 27.9 kHz for 4 cm water level, and at about 32.4 kHz for 3 cm liquid level. These values are considerably higher than the driving (20 kHz) or the typical large cavity oscillation (5 kHz). Furthermore, we see the structure also in other liquid containers, various submerged tip depths, and higher sonotrode frequencies.<sup>15,16</sup> Therefore, a resonant interaction of the attached cavity oscillation with the cuvette is unlikely. Altering the height of the fluid did however deteriorate the data from the hydrophone – more low amplitude oscillations were detected at small quantity of fluid – probably because of reflections from the free surface.

It was concluded that neither of the geometrical parameters influences the generation mechanism of the attached cavitation at the horn tip, as long as the liquid gap to the bottom is not too narrow. The self-generated large cavity oscillation frequency and the cavity’s extension did not change significantly for the tested range of geometrical parameters.

## V. DISCUSSION

The peculiar phenomenon of the large attached cavity at the horn tip, generating its own oscillation frequency in the subharmonic frequency range (i.e., lower than the driving frequency), turns out to be a quite robust phenomenon. All tested variations of liquid and geometric parameters did not significantly change either the appearance or the cavity's collapse frequency. This is in sharp contrast to the changes observed in the cavitation cloud of smaller bubbles further beneath the tip structure. These bubbles all show dependencies on liquid parameters that are well known for standard acoustic bulk cavitation.<sup>3</sup> For instance, bubbles become smaller for reduced surface tension, increase in number for smaller surface tension or higher temperature (higher vapor pressure), and they reduce in number for higher viscosity or lower gas saturation of the liquid. The independence of the large attached cavity with respect to liquid parameter variation points to a special type of acoustically induced cavitation. In particular, the irrelevance of dissolved gas content – apart from the inception phase, where smaller bubbles seem to be contributing – suggests an almost pure vapor cavitation at the tip. In other acoustic cavitation systems driven at 20 kHz, larger (mm-sized) bubbles are typically filled with non-condensable gas, result from degassing processes, and stay essentially passive (without strong collapse). Here, we observe a large vaporous cavity undergoing heavy collapse which highlights the relation of the phenomenon to hydrodynamic cavitation, although it is acoustically induced. Such systems might be termed “acoustic supercavitation.” This refers to the conjecture below that not the acoustic field itself, but the fast acceleration of the transducers surface might be the direct cause of nucleation. Furthermore, the radiating surface (the small tip) appears most of the time almost fully covered by the vaporous phase, which is somehow an analog to supercavitating bodies in a fast flow.<sup>6</sup>

In the following, we speculate on the physical mechanism behind the large attached structure.

In Ref. 6, an experiment on cavitation at accelerated (retracted) circular disks is reported, which bears some similarity to our observations.<sup>37</sup> Possibly the sufficiently fast retraction of the horn tip during its upward motion can create a large vaporous attached cavity which is too large for a collapse synchronously with the sound field. Potentially the large cavity develops from a merging of a ring (or vortex) cavity near the edges of the tip with a central cavity. Such a scenario appears to happen at the retracted disks for sufficient conditions.<sup>30</sup> With our side view imaging, we cannot definitely decide on this option for the horn tip, but the initial nucleation phase of the cavity as observed in Fig. 9 gives some indication that cavitation can start at the edges. Once the large cavity is formed, its subsequent dynamics is rather governed by the Rayleigh collapse time  $\tau = 0.915R_0\sqrt{\rho/p_0}$ , than by the acoustic driving period  $T = 1/f_0$ . Here,  $R_0$  is the initial radius of an empty spherical bubble,  $\rho$  the liquid density, and  $p_0$  the ambient pressure.<sup>2,3</sup> Indeed, when the observed attached cavity volumes of about 3–8 mm<sup>3</sup> (cf. Figs. 4–6) are re-calculated to simple spheres (or alternatively to attached half-spheres, which should have similar collapse times as full spheres in the bulk), we obtain equivalent radii of 0.9–1.2 mm (1.1–1.6 mm for the half-spheres). The self-generated frequency  $f^*$  would roughly correspond to the inverse of two Rayleigh collapse times,  $f^* = 1/(2\tau)$ , if we assume a symmetric expansion-collapse oscillation. We find a range of about 6000–4500 Hz (5000–3500 Hz for half-spheres), which is in reasonable agreement with the observations. Of course, deviations from (half-)sphericity, from temporal symmetry of expansion and collapse, and the influence of the oscillating sound pressure will lead to modifications of the calculation. For example, a closer inspection of the data shows typically a faster growth than collapse phase of the re-calculated vapor volume oscillation, together with a superposition of the acoustic period on the collapse side (but not on the expansion side). A coupling of sound pressure and/or tip motion to the cavity dynamics is apparent, not only in the volume modulations during collapse, but also because of the indications of entrainment/synchronization and period doubling. Still, the fundamental frequency can be significantly suppressed by the presence of the large cavity (compare also to Ref. 16 who sees a subharmonic peak larger(!) than the fundamental in the spectra). Further insight might be expected from a numerical treatment of the phenomenon, which is in preparation.

Let us stress again that the phenomenon of a large attached cavity is also robust to some amount with respect to setup geometry, horn frequency, and also horn tip erosion, as long as the tip diameter

is sufficiently small and/or the tip acceleration is large enough. For instance, a rough estimation of the maximum volume of the large cavity at the Branson horn tip in Fig. 1 leads to a value around  $14 \text{ mm}^3$  ( $R_0 = 1.5 \text{ mm}$  for a sphere and  $1.9 \text{ mm}$  for half-sphere) which yields an expansion-collapse cycle frequency of  $3.7 \text{ kHz}$  (spherical bubble) and  $2.9 \text{ kHz}$  (for half-spherical bubble), based on the same assumptions as above. This is a larger volume and smaller frequency than observed with the Bandelin horn, but is still in agreement with the observed cycle length frequency of  $3.3 \text{ kHz}$  (cf. Fig. 1).

The question remains at which parameters the cavitation switches from following the frequency of the horn to an attached large cavity of lower frequency oscillation, i.e., how and when the transition to “acoustic supercavitation” happens. We present several hypotheses why the cavitation oscillations cannot follow the horn frequency on a small horn, while they do on a bigger one:

- For decreasing horn tip diameter, typically the displacement amplitude grows, and thus the maximum acceleration. If the nucleation of “acoustic supercavities” is a function of (retractive) acceleration of a transducer surface, the small horn emitters would be more prone to this phenomenon. However, larger horns might be driven into large attached cavitation by still increased oscillation amplitude. As we have no more data on other horn accelerations for comparison yet, this stays speculation.
- On bigger horns there are always gaseous bubbles present on the tip because the flow cannot “wash” them away, or because acoustic forces drive them onto the surface.<sup>19,20</sup> The flow near the tip is therefore more compressible and pressure oscillations are reduced<sup>21</sup> – bubbles stay at a relatively small size and just follow the movement of the tip. On the contrary, on the small tip the gaseous bubbles can get washed away (see, for example, Fig. 10) what makes the flow momentarily less compressible. This might in turn cause large (negative) pressure excursions during a brief period, resulting in a very rapid nucleation and growth of larger vapor cavities in the vicinity of the horn or attached to it.
- At extended transducer surfaces, an attached large cavity might be more unstable than at a sufficiently small one, and thus disintegrate into smaller entities before covering the full tip. Indeed, directly on large emitter surfaces, localized cavitation cloud structures can occur (termed “smokers” in the literature<sup>10,19,38</sup>) which can partly – but not entirely – cover the surface.

Of course, one would like to quantify the transition to attached cavitation at the horn tip. As already mentioned, unsteady hydrodynamic cavitation shows vapor cloud shedding and resembles in some aspects the cavitation observed in the present experiment. Hence, a possible path is to employ the Strouhal number – a parameter, which is frequently used to characterize the dynamics of hydrodynamic cavitation.<sup>22</sup> If one takes the frequency of large cavity oscillation cycle  $f^*$ , the maximal velocity of the tip  $v_{\max}$ , and replaces the characteristic length by the cubic root of the maximal cloud volume  $V_{\max}$

$$Str = \frac{f^* \times \sqrt[3]{V_{\max}}}{v_{\max}}, \quad (2)$$

one gets  $Str = 1.40, 1.17,$  and  $0.94$  for the small ultrasonic tip at  $30\%, 50\%,$  and  $70\%$  power, respectively. A quite similar value  $Str = 0.75$  is obtained from the past study in Ref. 16 where similar (slow) cavitation dynamics on an ultrasonic horn with tip diameter of  $2 \text{ mm}$  and  $47.8 \text{ kHz}$  driving frequency was observed. The same calculation for a larger horn (Fig. 2(c)) gives a value of  $Str \approx 30$ . It is obvious that the values are significantly different and point to a simple way of characterizing the dynamics of cavitation on the ultrasonic horn tips. Interestingly, the Strouhal numbers found here to characterize the large attached cavitation structures with slow dynamics fall approximately in the same range as the ones which point to cavitation cloud shedding in hydrodynamic cavitation.<sup>22</sup>

## VI. CONCLUSIONS

By systematic measurements we investigated whether the peculiar dynamics of attached cavitation and self-generated cavity oscillation frequency on a small ultrasonic horn tip is a result of fluid properties. We observed the cavitation dynamics with synchronous high-speed imaging and

hydrophone recordings under variation of acoustic power, dissolved air concentration, liquid viscosity, surface tension, and temperature. The time resolved volume of the gas phase was calculated from the movie frames and could be related to the acoustic emissions. When the power of the transducer was held constant at 70%, but other parameters were varied, a clear constant frequency of the large cavity oscillation cycle was again and again measured – it corresponded to roughly 1/4th of the horn driving frequency (5 kHz cavitation frequency against 20 kHz driving frequency). The result is that obviously the fluid properties play no significant role in the dynamics of the attached cavitation on a small ultrasonic horn. A crucial influence of the setup geometry was also excluded (depth of horn submergence, liquid filling height in the cuvette) – here again a frequency of about 5 kHz was measured at 70% transducer power.

The observed large cavity cycle frequencies appear roughly consistent with a doubled Rayleigh collapse time cycle of expansion and collapse of equivalent spherical or half-spherical bubbles. The physical mechanism of large cavity generation at small tips, as opposed to large ones, was speculated upon with respect to transducer surface acceleration, bubble depletion at the surface, and large bubble stability. Calculation of an adapted Strouhal number (with cubic root of the volume instead of the length) revealed that, similar to hydrodynamic cavitation, values which are relatively low (around unity) characterize the dynamics of attached large cavities. In cases where the cavitation only occurs in streamers and clouds of smaller bubbles that follow the driving frequency, this value lies much higher (about  $Str > 20$ ).

In the spirit to distinguish the observed phenomenon with other cavitation dynamics at ultrasonic transducer surfaces, we suggest to term the observed phenomenon of attached cavities partly covering the full horn tip as “acoustic supercavitation.” This reflects the conjecture that not the sound field in terms of acoustic (negative) pressure in the liquid is responsible for nucleation, but the motion of the transducer surface.

## ACKNOWLEDGMENTS

We thank Viet Anh Truong from Hanoi University of Science and Technology for valuable discussions. Many thanks go to Jörg Enderlein and Qi Van from Drittes Physikalisches Institut, Göttingen University, for loan of equipment. The financial support by the Austrian Federal Ministry of Economy, Family and Youth and the Austrian National Foundation for Research, Technology and Development, and by Lam Research AG, Austria, is gratefully acknowledged.

- <sup>1</sup>E. A. Neppiras, “Acoustic cavitation,” *Phys. Rep.* **61**, 159 (1980).
- <sup>2</sup>F. R. Young, *Cavitation* (McGraw-Hill, London, 1989).
- <sup>3</sup>T. G. Leighton, *The Acoustic Bubble* (Academic Press, San Diego, 1994).
- <sup>4</sup>C. E. Brennen, *Cavitation and Bubble Dynamics* (Oxford University Press, New York, 1995).
- <sup>5</sup>W. Lauterborn and T. Kurz, “Physics of bubble oscillations,” *Rep. Prog. Phys.* **73**, 106501 (2010).
- <sup>6</sup>R. T. Knapp, J. W. Daily, and F. G. Hammitt, *Cavitation* (McGraw-Hill, New York, 1970).
- <sup>7</sup>Y. Lecoffre, *Cavitation Bubble Trackers* (Balkema, Rotterdam, 1999).
- <sup>8</sup>A. Eller and H. G. Flynn, “Rectified diffusion during nonlinear pulsations of cavitation bubbles,” *J. Acoust. Soc. Am.* **37**, 493 (1965).
- <sup>9</sup>T. G. Leighton, “Bubble population phenomena in acoustic cavitation,” *Ultrason. Sonochem.* **2**, S123 (1995).
- <sup>10</sup>R. Mettin, “Bubble structures in acoustic cavitation,” in *Bubble and Particle Dynamics in Acoustic Fields: Modern Trends and Applications*, edited by A. A. Doinikov (Research Signpost, Kerala, 2005), pp. 1–36.
- <sup>11</sup>R. Mettin, “From a single bubble to bubble structures in acoustic cavitation,” in *Oscillations, Waves and Interactions*, edited by T. Kurz, U. Parlitz, and U. Kaatzte (Universitätsverlag Göttingen, Göttingen, 2007), pp. 171–198.
- <sup>12</sup>M. Dular, R. Bachert, C. Schaad, and B. Stoffel, “Investigation of re-entrant jet reflection at an inclined cavity closure line,” *Eur. J. Mech. B/Fluids* **26**(5), 688–705 (2007).
- <sup>13</sup>T. Keil, P. F. Pelz, and J. Buttenbender, “On the transition from sheet to cloud cavitation,” in *Proceedings of the 8th International Symposium on Cavitation*, edited by C.-D. Ohl, E. Klaseboer, S. W. Ohl, S. W. Gong, and B. C. Khoo (Research Publishing, Singapore, 2012).
- <sup>14</sup>K. R. Laberteaux and S. L. Ceccio, “Partial cavity flows. Part 1. Cavities forming on models without spanwise variation,” *J. Fluid Mech.* **431**, 1–41 (2001).
- <sup>15</sup>R. Mettin, M. Dular, A. Znidarčič, and V. A. Truong, “Dynamics of attached cavitation at an ultrasonic horn tip,” in *Fortschritte der Akustik - DAGA 2012 Darmstadt*, Deutsche Gesellschaft für Akustik e.V., edited by H. Hanselka (DEGA, Berlin, 2012), pp. 447–448.
- <sup>16</sup>V. A. Truong, “A study of impulsive pressure distribution of cavitation generated by a high frequency vibrational probe,” *J. Sci. Technol. (Technical Universities Pub. Hanoi, Vietnam)* **73**, 78–84 (2009).

- <sup>17</sup> R. Esche, "Untersuchung der Schwingungskavitation in Flüssigkeiten," *Acustica* **2**, AB208 (1952).
- <sup>18</sup> E. A. Neppiras, "Subharmonic and other low frequency emissions from bubbles in sound irradiated liquids," *J. Acoust. Soc. Am.* **46**, 587 (1969).
- <sup>19</sup> A. Moussatov, R. Mettin, C. Granger, T. Tervo, B. Dubus, and W. Lauterborn, "Evolution of acoustic cavitation structures near larger emitting surface," in *Proceedings of the World Congress on Ultrasonics* (Société française d'acoustique, Paris, France, 2003), pp. 955–958.
- <sup>20</sup> C. Moussatov, C. Granger, and B. Dubus, "Cone-like bubble formation in ultrasonic cavitation field," *Ultrason. Sonochem.* **10**, 191 (2003).
- <sup>21</sup> K. Yasui, Y. Iida, T. Tuziuti, T. Kozuka, and A. Towata, "Strongly interacting bubbles under an ultrasonic horn," *Phys. Rev. E* **77**, 016609 (2008).
- <sup>22</sup> M. Dular and R. Bachert, "The issue of Strouhal number definition in cavitating flow," *J. Mech. Eng.* **55**(11), 666–674 (2009).
- <sup>23</sup> W. P. Mason and R. Wick, "A barium titanate transducer capable of large motion at an ultrasonic frequency," *J. Acoust. Soc. Am.* **23**(2), 209–214 (1951).
- <sup>24</sup> H. Kuttruff, *Physik und Technik des Ultraschalls* (Hirzel, Stuttgart, 1988).
- <sup>25</sup> E. A. Jackson, *Perspectives of Nonlinear Dynamics* (Cambridge University Press, Cambridge, 1991), Vol. 1.
- <sup>26</sup> R. Mettin, U. Parlitz, and W. Lauterborn, "Bifurcation structure of the driven van der Pol oscillator," *Int. J. Bifurcation Chaos* **3**, 1529 (1993).
- <sup>27</sup> R. Arndt, D. Kawakami, M. Wosnik, and M. Perlin, "Hydraulics," in *Springer Handbook of Experimental Fluid Mechanics*, edited by C. Tropea, A. L. Yarin, and J. F. Foss (Springer-Verlag, Berlin, 2007).
- <sup>28</sup> M. Dular, B. Bachert, B. Stoffel, and B. Širok, "Relationship between cavitation structures and cavitation damage," *Wear* **257**(11), 1176–1184 (2004).
- <sup>29</sup> J. Lee, M. Ashokkumar, S. Kentish, and F. Grieser, "Determination of the size distribution of sonoluminescence bubbles in a pulsed acoustic field," *J. Am. Chem. Soc.* **127**, 16810 (2005).
- <sup>30</sup> Y. Iida, M. Ashokkumar, T. Tuziuti, T. Kozuka, K. Yasui, A. Towata, and J. Lee, "Bubble population phenomena in sonochemical reactor: I. Estimation of bubble size distribution and its number density with pulsed sonication - Laser diffraction method," *Ultrason. Sonochem.* **17**, 473 (2010).
- <sup>31</sup> N. Segebarth, O. Eulaerts, J. Reisse, L. A. Crum, and T. J. Matula, "Correlation between acoustic cavitation noise, bubble population, and sonochemistry," *J. Phys. Chem. B* **106**, 9181 (2002).
- <sup>32</sup> C. Mishra and Y. Peles, "Flow visualization of cavitating flows through a rectangular slot micro-orifice ingrained in a microchannel," *Phys. Fluids* **17**, 113602 (2005).
- <sup>33</sup> J.-P. Franc, "Physics and control of cavitation," *Design and Analysis of High Speed Pumps*, Educational Notes RTO-EN-AVT-143, Paper 2, paper presented during the AVT-143 RTO AVT/VKI Lecture Series, von Karman Institute, Rhode St. Genèse, Belgium, 20–23 March, 2006, pp. 1–36.
- <sup>34</sup> C. Schaad, "Entwicklung und experimentelle Validierung eines Verfahrens zur Erweiterung der numerischen Kavitationsmodellierung," Ph.D. thesis, Technische Universität Darmstadt, Darmstadt, 2010.
- <sup>35</sup> H. Kato, M. Maeda, H. Kamono, and H. Yamaguchi, "Temperature depression in cavity," in *Proceedings of ASME Fluids Engineering Division Summer Meeting*, FED-Vol. 236 (ASME, 1996), Vol. 1, pp. 407–413.
- <sup>36</sup> A. Cervone, C. Bramanti, E. Rapposelli, and L. d'Agostino, "Thermal cavitation experiments on a NACA 0015 hydrofoil," *J. Fluids Eng.* **128**, 326–331 (2006).
- <sup>37</sup> L. J. Hooper, "Experimental investigation of initiation of cavitation behind an accelerated circular disk," in *Proceedings of the 1962 IAHR Symposium on Cavitation and Hydraulic Machinery*, edited by F. Numachi (International Association for Hydro-Environment Engineering and Research, Sendai, Japan, 1963), pp. 125–141.
- <sup>38</sup> L. Bai, C. Ying, C. Li, and J. Deng, "The structures and evolution of smoker in an ultrasonic field," *Ultrason. Sonochem.* **19**, 762 (2012).